

M. A Hierarchical, Structure-Oriented and Stochastic Approach to Model Liquid Molding Processes

Principal Investigator: Thanasis D. Papathanasiou

Department of Chemical Engineering

University of South Carolina

Columbia, SC 29208

Tel: 803-777-7219; fax: 803-777-6245; e-mail: papathan@enr.sc.edu

Technology Area Development Manager: Joseph A. Carpenter

(202) 586-1022; fax: (202) 586-1600; e-mail: joseph.carpenter@ee.doe.gov

National Science Foundation (NSF) Monitor: Mary Lynn Realff

This project was jointly funded by NSF and DOE

(703) 292-7088; fax: (703) 292-9056; email: mlrealff@nsf.gov

Contractor: University of South Carolina Research Foundation

Contract No.: DMI-0522221

Objective

To develop models for the hydraulic permeability of fibrous media, taking explicit account of the underlying microstructure and its variability. A specific task for the preceding period was to explain the scatter in the hydraulic permeability (K) of unidirectional random fiber arrays that is observed computationally as well as experimentally.

Approach

Our approach is computational. A large number of simulations have been carried out, using a parallel implementation of the Boundary Element Method (BEM), in microstructures consisting of ~600 fiber cross-sections placed within a containing unit-cell by a Monte Carlo (MC) procedure. This allows a direct and unambiguous correlation between (K) and the microstructure of the fiber arrays.

Accomplishments

- We find a reduction in (K) as the degree of local heterogeneity increases. This reduction follows a power-law, whose exponent is a linear function of fiber content.
- The hydraulic permeability (K) is a statistical function of the mean nearest inter-fiber spacing $\langle \delta_1 \rangle$
- The mean behavior of (K) can be expressed by the equation $\ln(\langle K \rangle / K_{hex}) / n = \ln(\langle \delta_1 \rangle / \delta_{hex})$, where n is a linear function of porosity and K_{hex} and δ_{hex} are also known functions of porosity.

Future Direction (for the next calendar year)

- Further optimize and develop parallel BEM code to run on a Dell cluster.
- Use this code to investigate the changes in (K) brought about by the transition of a microstructure from random to clustered. Develop explicit models that express changes in (K) in terms of microstructural parameters characterizing this transition.
- Directly link the stochastic character of (K) to the microstructural statistics of the fiber array.

- Modify the parallel BEM code to consider problems of linear, compressible elasticity. Use this code to predict the development of stress concentrations that characterizes the transition of uniform fiber arrays to arrays exhibiting various levels of small- and large-scale aggregation.
- Commence the development of a multipole-accelerated BEM code for Stokes flow.

Introduction

Viscous flow through fibrous media is a problem of long-standing interest in engineering due to its importance in the manufacturing and process industries. With specific reference to manufacturing of lightweight materials, flow through fibrous media is of direct relevance to several composites-forming operations such as liquid-molding, pultrusion and autoclave processing. To numerically model flow through fibrous preforms, nodal permeability values must be specified at points dictated by the domain discretization method; the accuracy in the provided permeability data is critical to successful modeling. For this purpose, permeability measurement techniques suitable for fibrous media similar to those used in liquid molding (preforms) have been developed. However, these measurements are known to be subject to large uncertainties, mainly caused by structural variations and/or deformation of the preform during the experiment. Therefore, in parallel with the development of more accurate and faster permeability testing methods, a great deal of effort has been devoted to developing models that would predict the permeability of a fibrous preform based on knowledge of its structure.

The present study is motivated by this need. The particular problem we consider is transverse flow through unidirectional, random fiber arrays. Large discrepancies are routinely observed between theoretical results for such arrays and experimental data obtained in real fiber beds. A notable feature of the permeability as measured in the latter is the substantial scatter in the measured values of (K). It has been widely assumed that these discrepancies are caused by the non-uniformity of real fiber beds. Indeed, fiber packing disorder, fiber bundling and fiber size variations are the norm in fiber preforms. Hence, it is not unreasonable that a function of porosity alone will not be sufficient to explain the observed variability in permeability data. Investigating the possible existence of structure-permeability correlations in disordered fiber arrays is therefore of obvious importance.

Problem Formulation

We consider a fibrous medium composed of long, cylindrical fibers with their axes oriented perpendicular to the direction of bulk flow. The computational unit cell represents a plane cut normal to the fibers' axes. As our focus is on the effect of the spatial distribution of fibers, these are of the same size. A typical unit cell is shown in Figure 1. The porosity of the system is $\phi = 1 - N_f \pi R^2 / A$, where N_f is the number of fibers, R is the fiber radius, and A is the area of the unit cell. The random configuration of fibers is generated by a MC procedure.

The governing equations for slow viscous Newtonian flow across the fibrous medium are the Stokes equations:

$$\nabla \cdot \mathbf{u} = 0 \quad \text{on } \Omega \quad (1)$$

$$\mu \nabla^2 \mathbf{u} = \nabla p \quad \text{on } \Omega \quad (2)$$

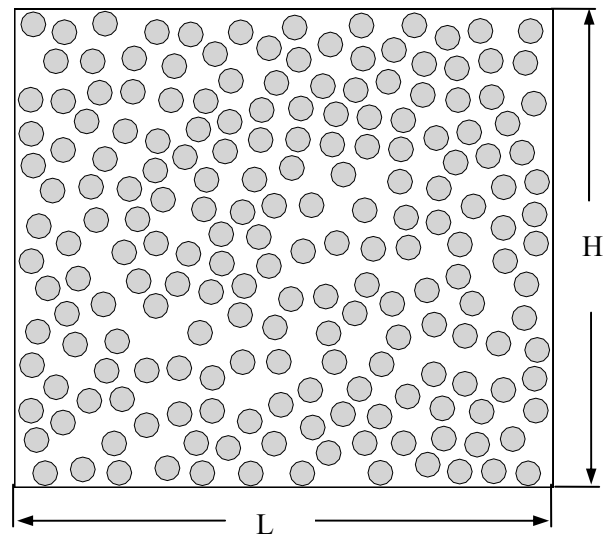


Figure 1. Model geometry used to represent a cross-section of a unidirectional array of randomly-placed fibers.

Here u , p , μ and Ω denote the velocity vector, pressure, viscosity and the 2-D flow domain, respectively. The governing equations can be cast into boundary integral representations involving boundary velocities and tractions only. This technique is well established. Using fundamental solutions, the boundary integral equations are usually written as:

$$c_{ij}(x_p)u_j(x_p) = \int_{\Gamma} u_{ij}^*(x_q, x_p)t(x_q)d\Gamma - \int_{\Gamma} t^*(x_q, x_p)u_i(x_q)d\Gamma \quad (3)$$

where u_{ij}^* is the Stokeslet representing the fluid velocity at x_p in the i^{th} direction due to a point force at x_q in the j^{th} direction and t_{ij}^* is the analogous singularity for tractions. Quadratic elements were used to discretize Eq.(3), providing second-order approximations for both geometry and field variables. After discretization, the resulting system of linear equations is usually represented as $[\mathbf{H}]\{\mathbf{u}\} = [\mathbf{G}]\{\mathbf{t}\}$, where $\{\mathbf{u}\}$ and $\{\mathbf{t}\}$ contain two complete sets of both known and unknown nodal velocity and tractions, respectively; and $[\mathbf{H}]$ and $[\mathbf{G}]$ are influence coefficient matrices whose elements are either non-singular or singular integrals. The non-singular integrals were typically evaluated by 10-point Gauss quadrature. The singular integrals were worked around by the well-known assumption of rigid-body motion, and the weakly-singular integrals were evaluated by Gauss-Laguerre quadrature with the aid of coordinate transformation. To prevent the deterioration of accuracy of numerical quadrature in non-singular integrals, the ratio of the closest distance between two nodes at different elements to the element size should be kept above a certain value. In the worst case, the closest distance between two nodes at different elements is equal to the minimum allowable, nearest inter-fiber spacing, δ_{min} . Therefore, the discretization of fiber surfaces should be finer when δ_{min} gets smaller. In this study, the smallest value of δ_{min} is one tenth of the fiber radius (R). We typically used 24-36 nodes per fiber. This translates to a distance-to-element ratio of 0.25 for less than 10^{-5} error according to an empirical error bound. It was observed that further refinement did not change the results significantly. Also specific to the problem setup, there is one

additional unknown of traction at each corner node. This has been treated using the stress balance method.

The main (inherent) shortcoming of the BEM is that its application results in dense and non-symmetric coefficient matrices. In the two-dimensional cases studied here, there are two unknowns for each node, plus four extra unknowns of traction at corner nodes because of the imposed boundary conditions, which result in $2 \times (N_f \times M_f + 4 \times M_b + 4)$ degrees of freedom, assuming M_f is the number of nodes per fiber and M_b is the number of nodes per unit-cell edge. The amount of computational work can exceed the capability of a workstation easily as the number of fibers in the unit cell increases. The bottleneck is the main memory (RAM) that can be used; for example, a simulation involving 576 randomly placed fibers results in a system with about 32,000 degrees of freedom and requires about 8 Gb of storage using double-precision arithmetic. For this reason, it is desirable to implement the BEM on a distributed-memory parallel computer. In this study, we implemented a parallel boundary element code which exploits the coarse parallelism in the different phases of the BEM, namely, matrix assembly, solution and post-processing. The solution of the dense linear system is the most time-consuming part in the BEM. In our study, the implementation of the L-U decomposition algorithm in ScaLAPACK is achieved using a two-dimensional block-cyclic data-decomposition scheme. This is scalable in the sense that the memory efficiency is N^2/np , where N is the global matrix size and np is the number of processors used. Our code was written in FORTRAN with function calls to BLACS, ScaLAPACK and MPI libraries.

Microstructure Generation and Quantification

The fiber distributions considered by this study were generated using a MC procedure, which is similar to the method described in Torquato's monograph¹ for generating an equilibrium ensemble of hard disks. The MC process starts with a fixed fiber packing arrangement (square array in our case) and proceeds

¹ Torquato, S. "Random Heterogeneous Materials," 1st edition, Chap. 12:273-277 (Springer-Verlag, 2001).

by randomly and sequentially perturbing the fiber locations. The microstructures generated in this manner are primarily governed by the choice of porosity ϕ and the minimum allowable inter-fiber distance δ_{\min} . The latter, defined as the closest distance between fiber surfaces, is the mechanism used to prevent fibers from overlapping during the MC process. Additionally, the unit-cell boundaries act like rigid walls to restrict fibers inside the cell. Such a MC process generates a random field which is short-range correlated. Typical fiber distributions generated in this manner are presented in Figure 2, with differences in ϕ and δ_{\min} . It is evident that small values of δ_{\min} result in patterns showing local (small-scale) fiber aggregation while large values of δ_{\min} lead to more or less uniform distributions that show only small deviations from a hexagonal lattice. The effect of δ_{\min} on fiber aggregation is more pronounced when the porosity is large. By varying δ_{\min} , a spectrum of fiber distributions can be generated at the same porosity level, ranging from locally aggregated to homogeneous. The possible range of δ_{\min} is determined by numerical considerations (at the low end) and by porosity (at

the high end). Specifically, the smallest value of δ_{\min} was taken to be one tenth of fiber radius (R) to ensure accurate integrations as well as to avoid excessive CPU time, as explained previously. In spite of the artificiality of this choice, we found that when δ_{\min} is given small values, the resulting fiber distributions appear similar to the ones we have observed in several liquid molded or pultruded unidirectional composites.

Prior to any analysis, it is necessary to quantify the microstructure of the fiber distribution first. In this effort, we have investigated the use of the nearest inter-fiber spacing — whose statistics differ between different fiber arrangements. For each fiber one can find a number of ‘neighbors’, which are assigned with a subscript (i) in such a way that the nearest one corresponds to $i=1$ and the others are in ascending order according to relative distances. Thus, the near-neighbor distances are the center-to-center distances from the reference fiber k to its neighbors, which are denoted as $\{d_i^k\}$. The nearest-neighbor distance for a reference fiber k is therefore the minimum in this distance set, i.e.,

$d_1^{(k)} = \min\{d_i^{(k)}\}$. For a population of fibers, the mean nearest-neighbor distance is denoted as $\langle d_1 \rangle$, which is simply an arithmetic mean. This metric is frequently used to indicate the degree of local heterogeneity in spatial point patterns. Small values of $\langle d_1 \rangle$ are associated with disordered patterns, while large $\langle d_1 \rangle$ indicate a homogeneous arrangement. By subtracting the fiber diameter D , d_1^k is translated to δ_1^k , which is the closest spacing between the reference fiber (k) and its neighbors. Because δ_1^k is more relevant to fluid space, we will use δ_1^k in correlating the microstructure of a fiber array to its permeability in the rest of this paper. We will also refer to the arithmetic mean of $\{\delta_1^k, k=1 \dots N_f\}$ as the mean nearest inter-fiber spacing, denoted as $\langle \delta_1 \rangle$.

As is the case in experimental measurement of permeability in fiber preforms, the stochastic nature of the fiber distribution leads to scatter in the computed permeability data. In this study, a number of random realizations (N_r) were generated for each class of fiber distributions characterized by ϕ and $\langle \delta_1 \rangle$ (or δ_{\min}), and the permeability values were

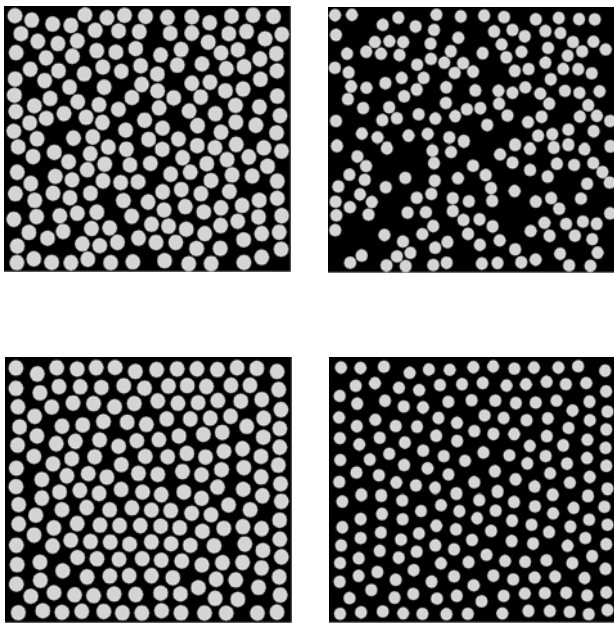


Figure 2. Sample geometries created by the MC process. They exhibit differing degrees of local aggregation. From top left clock-wise $(\phi, \delta_1) = (0.5, 0.1R)$; $(0.7, 0.1R)$; $(0.7, 1.0R)$; $(0.5, 0.4R)$

computed for the resulting unit cells. The average permeability and its standard deviation are then computed as:

$$\langle K \rangle = \frac{1}{N_r} \sum_i^{N_r} K_i \quad (4)$$

$$\sigma(K) = \frac{1}{N_r - 1} \sqrt{\sum_i^{N_r} (K_i - \langle K \rangle)^2} \quad (5)$$

Figure 3 shows one representative flow field computed for a unit cell containing 900 fibers using the parallel BEM code.

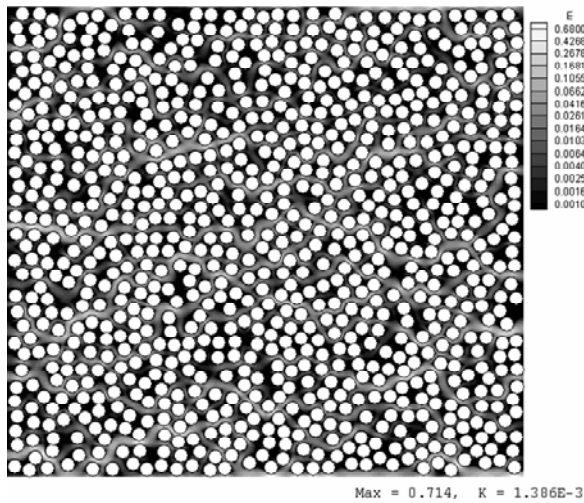


Figure 3. Fluid speed contours for slow viscous flows across a unidirectional fiber array consisting of 900 fibers at $\phi=0.50$. Flow is horizontal.

Results

The use of porosity alone is not sufficient to explain the scatter in the permeability of random fiber arrays, whether calculated numerically or determined by experiment. The objective of this study is to link the transverse permeability of random fiber arrays to the geometrical characteristics of these arrays. To do so, the dimensionless permeability data are plotted against $\langle \delta_1 \rangle / R$ in Figure 4. A correlation between K and $\langle \delta_1 \rangle$ is evident. In the porosity range $0.45 < \phi < 0.7$ it

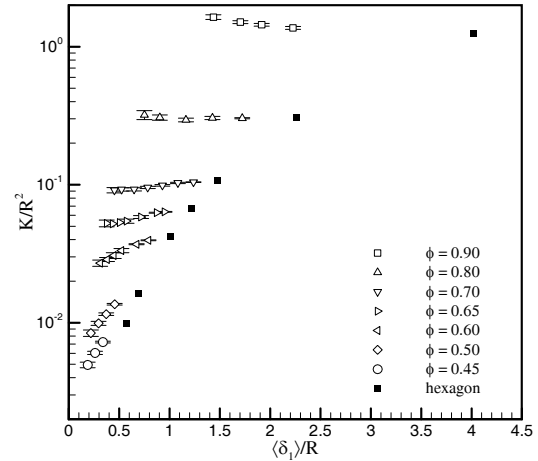


Figure 4. Correlation of the normalized permeability (K/R^2) with the mean nearest inter-fiber spacing, $\langle \delta_1 \rangle / R$. The symbols are mean values and the error bars represent standard deviations ($\pm \sigma$) in each ensemble of data. Each ensemble of data contains 20 runs on geometries of similar spatial statistics. Also shown are permeability values of hexagonal arrays.

appears that decreasing $\langle \delta_1 \rangle$ or, equivalently, moving from a homogeneous system to ones progressively showing higher local aggregation, results in a permeability reduction. This trend is more pronounced at lower porosities ($\phi = 0.45, 0.5$). This permeability reduction, as a result of non-uniformity in fiber distribution (quantified by the Morishita index in that case) was also reported in a recent study². At higher porosities, an opposite trend is shown: at $\phi > 0.7$ as $\langle \delta_1 \rangle / R$ decreases (below ~ 1.0 for $\phi = 0.8$), the permeability seems to increase. It is necessary to point out that large-scale clustering (in which cluster dimensions are comparable to unit-cell dimensions) does not occur in our systems because of the hard-core distribution statistics implicit in the MC procedure used for microstructure generation. The surprisingly good fit between $\langle \delta_1 \rangle$ and (K) can be qualitatively explained by the fact that, in the absence of large-scale clustering, the flow resistance around each fiber is governed by the narrowest gap separating it from its neighbors. The whole system can then be viewed as a network of flow paths connected in parallel as well as in series. The resistance of each component in the network is

² Bechtold, G. and Ye, L. Compos. Sci. Technol. 63:2069-2079 (2003).

determined by the narrowest gap, which is included in the statistics of the inter-fiber spacing (see earlier section). It is therefore not surprising that such a clear correlation exists between $\langle \delta_1 \rangle$ and $\langle K \rangle$.

In the porosity range of practical interest to composites manufacturing ($0.45 < \phi < 0.70$), Figure 4 suggests that the functional form which describes the relation between $\langle \delta_1 \rangle$ and K should be:

$$\frac{K}{R^2} = \left(\frac{\langle \delta_1 \rangle}{R} \right)^n f(\phi) \quad (6)$$

where the exponent n is a function of ϕ as evidenced by the different slopes of the data sets corresponding to different porosities. In seeking a functional form for $f(\phi)$ in Eq.(6), we recall that Eq.(6) should reduce to existing models for the transverse permeability when the fiber array becomes uniform. When the array approaches a uniform hexagonal array, $\langle \delta_1 \rangle$ should equal the inter-fiber spacing of a hexagonal array (δ_{hex}) and the corresponding permeability will be K_{hex} , which is known to be only a function of porosity. For example, at the low porosity limit, K_{hex} and δ_{hex} are given by Eq. (7):

$$K_{hex} = \frac{2}{9\pi\sqrt{3}} \left(\frac{\delta_{hex}}{R} \right)^{5/2} R^2 \quad (7a)$$

$$\delta_{hex} = 2 \left(\sqrt{\frac{1-\phi_{min}}{1-\phi}} - 1 \right) R \quad (7b)$$

where $\phi_{min} = 1 - \pi/(2\sqrt{3})$, is the porosity at maximum packing for a hexagonal array. To be asymptotically correct, the form of $f(\phi)$ should therefore be:

$$f(\phi) = \left(\frac{R}{\delta_{hex}} \right)^n \frac{K_{hex}}{R^2} \quad (8)$$

and thus Eq.(9) yields:

$$\frac{K}{K_{hex}} = \left(\frac{\langle \delta_1 \rangle}{\delta_{hex}} \right)^n \quad (9)$$

We attempted to scale the computational results of Figure (4) as suggested by Eq. (9). The result is presented in Figure 5(a), in which each data point corresponds to one simulation, characterized by one set of values $(\phi, \langle \delta_1 \rangle)$. As expected by the dependence of the exponent n on ϕ , this scaling does not collapse the data onto one single master curve. Fitting the data as a power function gives the lowest estimate of $n=0.164$ at $\phi=0.7$ and the highest estimate $n=0.628$ at $\phi=0.45$. It is interesting to note that a plot of n versus ϕ suggests a linear relationship $n=\alpha+\beta\phi$. Therefore an overall correlation between K and $\langle \delta_1 \rangle$ for random fiber arrays can be written as:

$$\frac{K}{K_{hex}} = \left(\frac{\langle \delta_1 \rangle}{\delta_{hex}} \right)^{\alpha+\beta\phi} \quad (10)$$

where the constants α and β are determined from a least square fit as $\alpha = 1.51 \pm 0.06$ and $\beta = -1.93 \pm 0.10$. It goes without saying that the linear relationship $n = \alpha + \beta\phi$ can only be considered applicable in the indicated range of ϕ and $\langle \delta_1 \rangle$. Taking logarithms in both sides of Eq. (10) results in:

$$\ln(K/K_{hex})/n(\phi) = \ln(\langle \delta_1 \rangle/\delta_{hex}). \quad (11)$$

The computational data for (K), transformed according to Eq. (11), are plotted in Figure 5 (b). A solid line in Figure 5(b) indicates the least square fit of the data set to a linear model with slope around unity (0.994 ± 0.018) and intercept (-0.008 ± 0.01) very close to zero, exactly as anticipated from Eq.(11). It seems that Eq.(11) predicts the correct average behavior, as the data are indeed shown to be distributed randomly around an average log-linear relationship. In the studied ranges of ϕ and $\langle \delta_1 \rangle$, the permeability follows, on average, Eq. (11), with a scatter that is inversely proportional to $\langle \delta_1 \rangle$. Additionally, the scatter of the permeability values around the mean trend is also related to the variance (σ^2) of δ_1 , or, in other words, to the non-uniformity

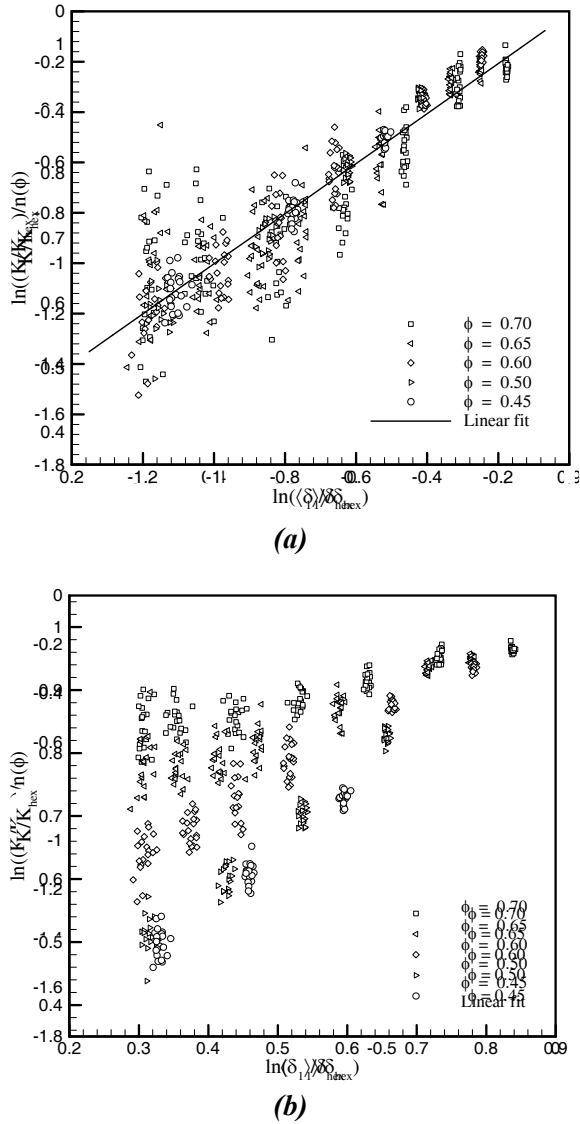


Figure 5. The correlation between permeability and the mean nearest inter-fiber spacing in the porosity range [0.45, 0.70]: (a) plot of the reduced permeability (K/K_{hex}) versus $\langle\delta_1\rangle/\delta_{hex}$; (b-bottom) plot of $\ln(K/K_{hex})/n$ versus $\langle\delta_1\rangle/\delta_{hex}$. Each data point in the graph is the result of one simulation. The linear fit in (b) has a slope of (0.994 ± 0.018) and an intercept of (-0.008 ± 0.01) .

of the underlying microstructure. Relating the known statistics of (δ_1) to the obtained statistics of (K) is of great practical interest and we are working in this direction.

Conclusion

We carried out an extensive investigation of Stokes flow across a large number of unidirectional, random fiber arrays generated by a MC procedure. This numerically-intensive task was accomplished by developing and running an in-house parallel boundary element code on a distributed-memory parallel computer. The transverse permeability (K) of systems consisting (each) of 576 fibers, calculated in the porosity range $0.45 < \phi < 0.90$ by averaging over 20 random realizations at each porosity value, was computed. Following this, we point out the need to consider some measure of the underlying fiber spatial statistics as an additional parameter affecting permeability. The microstructural characteristics of the model fiber distributions were analyzed and the mean nearest inter-fiber spacing $(\langle\delta_1\rangle)$ was identified as a parameter that correlates with the numerical estimates of (K) . Specifically, we found that (K) is a statistical function of $(\langle\delta_1\rangle)$, with its average behavior $(\langle K \rangle)$ expressed by $\ln(\langle K \rangle / K_{hex}) / n = \ln(\langle\delta_1\rangle / \delta_{hex})$, where (n) is a linear function of porosity and K_{hex} and δ_{hex} are also known functions of porosity. The deviation of (K) from this average behavior is related to the variability of the underlying microstructure, as expressed by the variance of (δ_1) .

Presentations/Publications/Patents

X. Chen and T.D. Papathanasiou, 'Understanding the scatter in the permeability of random fiber arrays: A statistical correlation in terms of mean inter-fiber spacing', subm. Physics of Fluids, 10/2005.